Particle Accelerators
1976, Vol. 7, pp. 137–150

STANFORD'S SUPERCONDUCTING HEAVY ION LINAC STUDY: The Triple Focusing Linear Accelerator†

E. E. CHAMBERS and I. BEN-ZVI‡

High Energy Physics Laboratory, Stanford University, Stanford, California 94305, USA

(*Received September 24, 1973; in final form May 29, 1974*)

Alternating phase focusing is investigated. Parameters for two successive accelerator sections taking $^{35}Cl^{+8}$ from $\beta = 0.030$ to $\beta = 0.075$ and then to $\beta = 0.127$ are numerically calculated and compared with theory. Effects of varying the parameters and of phase adjustment errors are also considered.

1 INTRODUCTION

In a linear accelerator a group of ions that is ahead of the maximum accelerating phase is bunched but defocused, a group behind the maximum is focused but debunched. A group that alternates between these conditions can be overall bunched, and focused in both transverse directions; hence focused by the rf field in all three directions.

Much has been written[1–5] in the last 20 years about such a system but, because of the cost of such a system built at 300°K and its relatively small acceptance, little effort has been put into a real triple focusing accelerator.

The superconducting heavy ion linac offers an excellent opportunity to make use of a triple focusing system, for the following reasons:

a) One advantage of a cryogenic linac is the high beam quality possible. This necessitates limiting the beam phase space, therefore we are not interested in a large phase acceptance.[6] Bunching the injector beam, where the injector to the linac section is a Tandem Van der Graaff, introduces an energy spread which is best dealt with through debunching following the linac. In this situation we accept a small phase spread, and a large energy spread. The triple focusing linac has this property, as one can see from the final results of this work.

b) The gaps of the cryogenic linac are independently controlled. This is made possible by the low rf power and the long time constant of the cavities which brings the cost of the electronics down. Thus the option of alternating phase focusing will be built in, justifying a closer look of this method.

c) The acceptance in a heavy ion cryogenic linac is larger than, say, a room-temperature proton linac, on account of the larger accelerating field and the lower ion velocity βc. This follows the focusing power being proportional to the accelerating field, and to β^{-3}. In our linac development project we investigated both alternating phase focusing and quadrupole focusing. This report covers the first approach, while the other will be reported later in this series. However, it seems likely that, taking advantage of the independent gap phasing, the linac will incorporate both focusing methods, having quadrupole lenses assisted by a varying degree of alternating phase focusing. In this work the properties of two triple focusing accelerators at different frequencies are considered. The theoretical acceptance is considered and then a model beam and accelerator are set up and defined by parameters as nearly orthogonal as possible. The parameters are varied to find the optimum set. It is considered optimum when the input multidimensional phase space volume is as large as possible while nearly 100% of its content traverses the entire accelerator. The effect of varying some other parameters will also be considered. The specialized questions of focusing strength choice, time-of-flight factor, and energy gain dependence on r are considered as well.

† Work supported by the National Science Foundation under Grant No. GP33411.

‡ Presently on leave from the Weizmann Institute of Science, Rehovoth, Israel.

2 THEORETICAL ACCEPTANCE

The question now to be answered is "what will be the maximum acceptance of such an accelerator and how will it be attained?" This problem was approached in another paper by one of the authors.[5] That work or other sources for beam dynamics should be consulted for details that are skipped here for brevity.

The energy gain of an ion in a particular cell is

$$\Delta K = qWT(k)I_0(ar)\cos\phi \tag{1}$$

where q is the charge on the ion
W is the maximum potential difference across the cell
T is the time of flight factor
I_0 is the modified Bessel function
$k = 1/\beta\lambda$
$a^2 = k^2 - 1/\lambda^2$
$\phi = \phi_s + \psi$
ϕ_s is the synchronous phase
ψ is deviation from synchronous phase
r is distance off axis

and T has the form

$$T(k) = \frac{\sin(gk/2)}{(gk/2)I_0(aR)} \tag{2}$$

if the axial electric field is uniform over the gap g at a distance R off axis, and is zero otherwise at a distance R off axis.

In traversing a cell there will be focusing if the group of ions arrives after the phase of maximum acceleration, in which case the phase of those ions is here defined to be negative. The focusing is characterized by the focusing power

$$-\frac{\Delta r'}{r} = \delta_r \tag{3}$$

and

$$\delta_r = -\tfrac{1}{2}\delta_0 H U_r, \tag{4}$$

where

$$\delta_0 = \frac{qWT\sin\phi_s}{\lambda mc^2\beta^3\gamma^3} \tag{5}$$

$$H = I_1\frac{(ar)}{(ar/2)} \approx 1 + \frac{(ar)^2}{8}, \tag{6}$$

$$U_r = \frac{\sin\phi}{\sin\phi_s} \approx 1 + \psi\cot\phi_s. \tag{7}$$

Similarly there will be bunching if $\phi_s > 0$

$$-\frac{\Delta\psi'}{\psi} = \delta_z \tag{8}$$

and

$$\delta_z = \delta_0 I_0 U_z, \tag{9}$$

where

$$I_0(ar) \approx 1 + \frac{(ar)^2}{4}, \tag{10}$$

$$U_z = -\frac{\cos\phi - \cos\phi_s}{\psi\sin\phi_s} \approx 1 + \frac{\psi}{2}\cot\phi_s. \tag{11}$$

If ψ and (ar) are small, the nonlinearity of the Bessel functions and sinusoids may be ignored and the functions, H, U_r, I_0, U_z whose difference from unity characterize those nonlinearities may be set to unity. Further, the similarity of Eqs. (3) and (8) above shows that both bunching and focusing may be treated by the same formalism. Hence,

$$-\frac{\Delta x'}{x} = \delta \tag{12}$$

where x stands for either r or ψ. If there are n focusing/defocusing cells the matrices

$$F^n = \begin{pmatrix} \cos(n\theta) & l\sin(n\theta) \\ -\frac{1}{l}\sin(n\theta) & \cos(n\theta) \end{pmatrix}$$
$$D^n = \begin{pmatrix} \cosh(n\theta) & l\sinh(n\theta) \\ \frac{1}{l}\sinh(n\theta) & \cosh(n\theta) \end{pmatrix} \tag{13}$$

will transform the matrix of the ion

$$X = \begin{pmatrix} x \\ x' \end{pmatrix} \tag{14}$$

through those cells where

$$\theta^2 = L\delta \tag{15}$$

$$l^2 = \frac{L}{\delta} \tag{16}$$

and

$$L = \text{length of cell.} \tag{17}$$

The assumption that led to Eqs. (15) and (16) is that the impulse applied to a cell is uniformly distributed throughout its length *or* that

$$\theta^2 \ll 1. \tag{18}$$

If there are $n/2$ focusing cells, n defocusing cells, and another $n/2$ focusing cells in that order the matrix that transforms X can be written as

$$P = F^{n/2}D^nF^{n/2} = \begin{pmatrix} \cos\Omega & B\sin\Omega \\ -\frac{1}{B}\sin\Omega & \cos\Omega \end{pmatrix}, \tag{19}$$

where

$$\cos\Omega = \cosh(n\theta)\cos(n\theta) \tag{20}$$

$$\frac{B}{nL} = \frac{\cosh(n\theta)\sin(n\theta) + \sinh(n\theta)}{(n\theta)\sin\Omega}. \tag{21}$$

The condition for overall focusing is that $0 < \Omega < \pi$, or

$$0 < (n\theta)^2 < 3.516. \tag{22}$$

If the ion beam before it is transformed by P can be represented by an erect ellipse in x, x' space of dimensions x_0 and x_0', and if the beam has been properly shaped so that

$$\frac{x_0}{x_0'} = B, \tag{23}$$

then P will transform the original beam ellipse into itself and the maximum excursion will be minimized for a given acceptance. The acceptance is measured by the product (x_0, x_0') and assuming a properly Eq. (23) shaped beam,

$$x_{\max} = [B(x_0, x_0')]^{1/2}. \tag{24}$$

In order to minimize the maximum excursion for a given acceptance, B should be small.

Another quantity is the modulation ratio, the ratio between the $x_{\max}$ at the center of a focusing section and $x_{\max}$ at the center of a defocusing section. It is given by

$$Q = \left(\frac{\sinh(n\theta) + \sin(n\theta)\cosh(n\theta)}{\sin(n\theta) + \sinh(n\theta)\cos(n\theta)}\right)^{1/2}. \tag{25}$$

The functions Ω, B/nL, and Q are plotted in Figure 1 as a function of $(n\theta)^2$. The points marked on the B/nL curve correspond with the choice of $(n\theta_z)^2 = 2.9$ and, necessarily therefore [the "$\frac{1}{2}$" in Eq. (4)], $(n\theta_r)^2 = 1.45$, which nearly minimizes

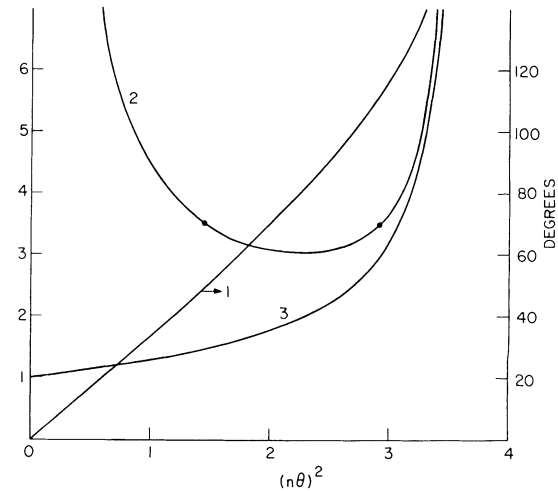

FIGURE 1 (1) Ω, (2) B/nL, and (3) Q *vs* $(n\theta)^2$.

both B_z and B_r. From first order considerations these appear to be good operating conditions.

In the first order system so far considered, there is no limit on acceptance. However, the nonlinearity of sinusoids and Bessel functions must be considered. It is convenient to consider first the effect of ψ acceptance on stability through Eqs. (7) and (11). Since ψ is near its maximum magnitude for a relatively long time and ϕ_s changes its sign comparatively rapidly, both Eqs. (7) and (11) can be rewritten in the form

$$U_\pm = 1 \pm \alpha \tag{26}$$

in which the upper sign is associated, say, with the focusing (or bunching) and the lower sign with the defocusing (or debunching).

During the focusing (or bunching) $\delta_+ = \delta_0 U_+$ and during defocusing (or debunching) $\delta_- = \delta_0 U_-$, where δ_0 is the value of δ for $\alpha = 0$. Similarly to obtain the matrix F, these values would be determined

$$\theta_+ = \theta_0\sqrt{U_+}, \qquad l_+ = \frac{l_0}{\sqrt{U_+}} \tag{27}$$

For the matrix D the minus sign would be used. The matrix P is unchanged in form, but the definitions of Ω and B become more complicated:

$$\cos\Omega = \cosh(n\theta_-)\cos(n\theta_+) + C_0\sinh(n\theta_-)\sin(n\theta_+), \tag{28}$$

$$\frac{B}{nL} = \frac{\cosh(n\theta_-)\sin(n\theta_+) - C_0 \sinh(n\theta_-)\cos(n\theta_+) + C_1 \sinh(n\theta_-)}{(n\theta_+)\sin\Omega} \quad (29)$$

where

$$C_0 = \frac{\left[\left(\frac{U_-}{U_+}\right)^{1/2} - \left(\frac{U_+}{U_-}\right)^{1/2}\right]}{2}$$

$$C_1 = \frac{\left[\left(\frac{U_-}{U_+}\right)^{1/2} + \left(\frac{U_+}{U_-}\right)^{1/2}\right]}{2}$$

and the reciprocal of the modulation ratio is given by

$$\frac{1}{Q} = \left[\cosh(n\theta_-)\cos(n\theta_+) - \left(\frac{U_+}{U_-}\right)^{1/2} \sinh(n\theta_-)\sin(n\theta_+)\right]^2 + \frac{1}{B^2}\left[l_+ \cosh(n\theta_-)\sin(n\theta_+) + l_- \sinh(n\theta_-)\sin(n\theta_+)\right]^2. \quad (30)$$

The above relations are shown graphically in Figure 2 which is similar to the stability curves of Smith and Gluckstern concerning quadrupole focusing. There are three sets of curves on Figure 2. The small-dashed curves are for constant Ω. Between $\Omega = 0$, the 0 mode, and $\Omega = \pi$, the π mode, Ω is real and there is stability. Outside these bonds Ω is imaginary and the excursions are unbounded. The solid curves are for constant $B/nL = 2$, 3, 4, 5, and 10. B approaches infinity as the instability of the 0 or π mode is approached, but it should be noted that even very close to instability B increases by only a factor of 3 greater than its least value on the axis. Ω and B/nL on the $(n\theta)^2$ axis are given by curves 1 and 2 of Figure 1. The third set of curves on Figure 2 is the dashed set for constant modulation ratios of $Q = 1.5$, 2, and 3.

Now the question is what is the maximum value of ψ that is consistent with stability and what is the corresponding value of $(n\theta_\phi)^2 = 2(n\theta_r)^2$. The bottom of Figure 3 is a reproduction of Figure 2 with only the limits of stability shown. The bar AB represents a bunch travelling to the right. The curve above it represents the accelerating force given to the various parts of the bunch in the bunching part of the cycle. The line segment $A'B'$ between the limits of stability corresponds with the bunch AB and delineates the range of stability insofar as phase is concerned. The curve below the bar indicates the focusing force during the

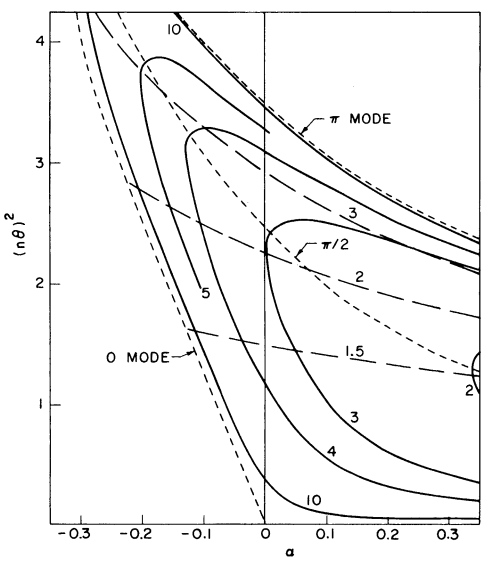

FIGURE 2 Stability, modulation and mode curves in the $(n\theta)^2 - \alpha$ space.

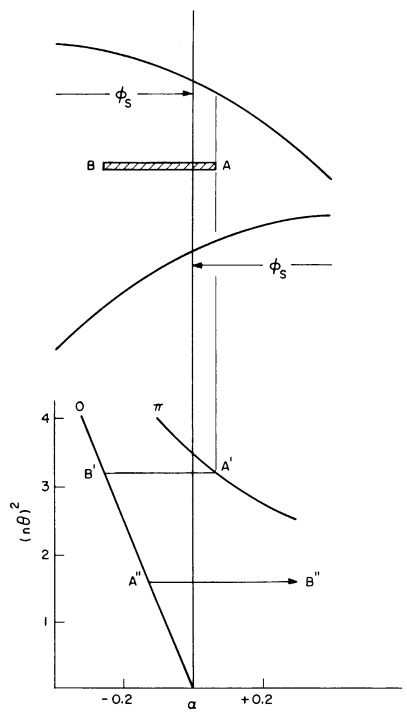

FIGURE 3 Limits of stability of the phase bunch.

focusing part of the cycle. The sign of ψ for any particle in the bunch is now reversed so when considering the focusing stability the bar AB must be reflected about the line $\alpha = 0$. Furthermore, by comparing Eqs. (7) and (11) it will be seen that α_r will be twice as great α_ϕ for the same ψ, so double the size of the bar. By dropping perpendiculars we locate the limits of stability $A''B''$. The initial choice of the location of the point A on the bar such that $\alpha(A'') = -2\alpha(A')$. From Eqs. (7) and (11) we get

$$\alpha(B') = \tfrac{1}{2}\psi_- \cot \phi_s$$
$$\alpha(A') = \tfrac{1}{2}\psi_+ \cot \phi_s$$
$$\alpha(A'') = -\psi_+ \cot \phi_s.$$

Thus the maximum phase excursions ψ_+ and ψ_- are given in terms of the values of α at the stability lines. $\alpha(A')$ and $\alpha(A'')$ determine ψ^+ the maximum phase excursion in the focusing (or bunching) section, for phase and radial stability respectively, while $\alpha(B')$ determines the limit on ψ_-, and thus the phase acceptance is determined.

Radial acceptance affects the energy gained and focusing power through the Bessel functions as indicated in Eqs. (1) and (6) respectively. The most stringent condition is simply keeping the energy gain within bounds. Setting the bounds is not so simple, however, and we have to make some simplifying assumptions. The middle of the bunching section at which point most of the calculations are made has the minimum energy excursions. At the middle of the debunching section it is increased by the modulation ratio. However it is largest at the interface between the bunching and debunching sections, although these excursions are highly correlated with the phase excursions. If the maximum radial acceptance is assumed to be r_0 and the standard energy gain at $r_0/\sqrt{2}$ then the excursion caused by this spread in accordance with Eq. (10) in one cell is $\Delta\varepsilon = \frac{1}{8}\Delta K/K(r_0/\beta\lambda)^2$. In $n/2$ cells if this accumulation of $\Delta\varepsilon$ is set equal to the minimum excursion times the appropriate modulation factor for the interface all the information is available to calculate the upper bound on R. To get estimates of the acceptance, we have to choose proper values for some parameters.

One of the fundamental parameters to choose in a triple focusing accelerator is the value of $(n\theta_z)^2 = n^2 L\delta_z$, where n is the number of cells in a row that are bunching or debunching, L is the length of a cell, and δ_z is the bunching power of a single cell. From a first order argument and from maximizing the expected acceptance it appeared that the best choice was $(n\theta_z)^2 = 2.9$.

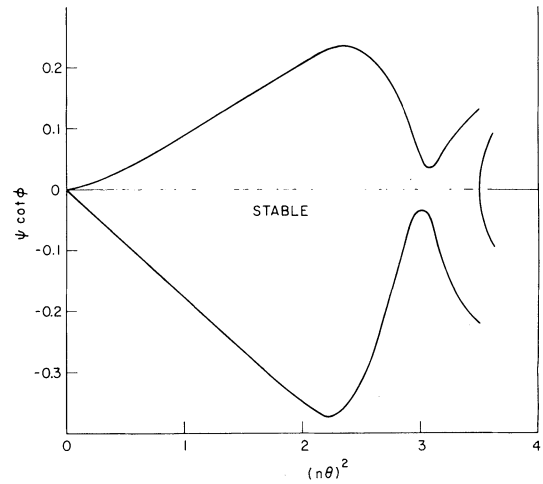

FIGURE 4 On axis stability *vs* bunching power.

It turns out that this is very nearly the worst possible choice due apparently to the fact that $(n\theta_z)^2 = 3.03$ corresponds with the $\Omega = 2\pi/3$ mode as can be seen in Figure 1. The other integer-related modes, e.g. $\Omega = \pi/2$ at $(n\theta_z)^2 = 2.47$, are not significant as is shown in Figure 4. This figure is generated using on-axis ions, the continuous (difference in) impulse approximation without net acceleration and an accelerator of length 30 nL. The ordinant refers to the initial value of ψ and is as shown because the equations of motion depend on $\psi \cot \phi_s$ as long as $\psi^2/6 \ll 1$. The figure is drawn for $\cot \phi_s = 2$ and checked at arbitrary abscissas for $\cot \phi_s = 1$. Except for the arbitrary length the figure is generally applicable for reasonable values of ϕ_s. It indicates a maximum phase acceptance at $(n\theta_z)^2 = 2.25$ with $\psi_+/\psi_- = 0.62$. This is for $r = 0$, but explains the sharp fall of acceptance as $(n\theta_z)^2$ approaches 3.0. Now using the outlined procedure to calculate the stability limits on the phase and radial excursions, we find that the limit of excursions should be about

$$\psi_0 = 0.15 \tan \phi_s \tag{31}$$

$$r_0 = 0.5\beta\lambda \tan \phi_s \tag{32}$$

and that the ratio of the maximum phase excursion ahead of the synchronous particle to the maximum excursion behind should be about

$$R_\psi \equiv \frac{\psi_{+\max}}{\psi_{-\max}} \approx 0.62. \tag{33}$$

for maximum acceptance. It was also shown that

for maximum acceptance the limit values of ψ' and r' should be chosen as

$$\psi'_0 = \frac{\psi_0}{B_z} \tag{34}$$

and

$$r'_0 = \frac{r_0}{B_r}. \tag{35}$$

These values of ψ_0 and ψ'_0 are based on the assumption that the accelerator starts in the middle of a bunching section. Similarly the values of r_0 and r'_0 are based on starting it in the middle of a focusing section. Since focusing is available outside the accelerator the arbitrary choice was made to start with a section that is bunching but defocusing. In this case r_{max} and r'_{max} must be multiplied and divided, respectively, by the modulation ratio Q.

3 COMPUTER CALCULATIONS

The calculation of individual ion orbits is accomplished in a program called ZRFOCUS and is based on fields determined by the LALA[7] program. Ideally a highly accurate integration subroutine would be used. However, such a subroutine requires a lot of time to run because the interpolating required in the two dimensional LALA output must yield smooth fields for the integrating subroutine which tends to take an excessive number of steps at irregularities.

The highly accurate integrating subroutine is not necessary if care is taken to assure equivalent treatment of each ion. The equivalence is obtained by integrating for the variables E, ψ, r, r', with a fixed Δz such that no interpolation in z is required and that interpolation in r is smooth enough.

The LALA output was for a total field length of 68 mm (the gap was 10 or 20 mm), but the length of integration was cut to 64 mm. With $\Delta z = 16$ mm, the integration output was next to meaningless; at 8 mm it was meaningful, at 4 mm it was deemed to be sufficiently accurate, and at 2 and 1 mm the integration appeared to be accurate.

A fictitious sinusoidal LALA field was generated, processed like the real field, and gave the closed form results for $\beta \sim 1$. The sinusoidal field also confirmed that $\Delta z = 4$ mm was sufficiently accurate.

The LALA output is in the tabular form $F(r, z) = rB_\theta$ (where B_θ stands for the magnetic field multiplied by λc in mks units), for r and z in steps of 1 mm. The required fields are:

$$\begin{aligned} B_\theta &= \frac{F}{r} \\ E_r &= \frac{1}{r}\frac{\partial F}{\partial z}. \\ E_z &= \frac{1}{r}\frac{\partial F}{\partial r} \end{aligned} \tag{36}$$

But near the axis where it is of most interest the form of F is

$$F = f_1(z)r^2 + f_2(z)r^4 + \cdots$$

which suggests defining a new function

$$\begin{aligned} G &= \frac{F}{r^2} \text{ generally and} \\ &= \frac{1}{2}\frac{\partial^2 F}{\partial r^2} \text{ at } r = 0 \end{aligned} \tag{37}$$

which has the form

$$G = g_1(z) + g_2(z)r^2 + \cdots$$

and is a much better behaved function than F, hence simplifying interpolation. Now the fields have the form

$$\begin{aligned} B_\theta &= rG \\ E_r &= r\frac{\partial G}{\partial z} \\ E_z &= 2G + r\frac{\partial G}{\partial r} \end{aligned} \tag{38}$$

and interpolation is very easy when there are only a (small) finite number of values of z.

Since there are only a few values of r in the table, predetermination of all interpolation coefficients will speed the final integration calculation. At each z we need to find sets of coefficients A_{ki} and B_{ki} such that

$$\begin{aligned} G(r_k + \Delta r) &= \sum_{i=1}^{4} A_{ki}\Delta r^{i-1} \\ \frac{\partial G}{\partial z}(r_k + \Delta r) &= \sum_{i=1}^{4} B_{ki}\Delta r^{i-1} \end{aligned} \tag{39}$$

Operationally we start with LALA output of F for $z = 0$ to 34 and $r = 0$ to 10 for each integer

(in millimeters), and generate the even function F so that appropriate derivatives at $z = 0$ and $r = 0$ will correctly be evaluated as zero. Now this tabulated function F is referred to the subroutine DCS2ME of the International Mathematics and Statistics Library, Stanford University, to obtain $\partial^2 F/\partial r^2$ at $r = 0$. Now the tabulated function G is generated in accordance with its definition Eq. (37) and then G is referred to the same subroutine to obtain $\partial G/\partial z$ as another tabulated function.

Each of the functions G and $\partial G/\partial z$ is referred to subroutine SPLINE of the Computer Science Department, Stanford University, to obtain the coefficients A_{ki} and B_{ki} of definitions Eq. (39). The coefficients used are for $z = 0$ to 32 and $r = 0$ to 9.

The SPLINE subroutine makes the function and the first two derivatives continuous in r. Since E_z is generated by taking a derivative in r, it is the least smooth, but still E_z and $\partial E_z/\partial r$ will be continuous which is more than smooth enough.

With G being a slowly varying function the fields can be determined from Eqs. (38) and (39) consistently, rapidly, smoothly and accurately as the initial LALA data permit.

The LALA outputs actually used were calculated for two re-entrant cavities, one at 217 MHz and one at 433 MHz. The cavities in the vicinity of the beam line, are shown in Figure 5.

The program ZRFOCUS traces the path of ions through a repetition of identical cells, each cell being made up of a drift, a length in a field according to LALA, and a second drift equal to the first.

First ZRFOCUS determines the phase and energy of the synchronous ion throughout the length of the accelerator by, for each cell,

1) integrating through the cell to obtain its bunching power at the approximately correct phase,

2) calculating the correct phase to get the specified value of the bunching power and

3) integrating again for the final energy at the correct phase.

At the beginning of each group of n cells a perhaps new value of n is calculated such that the value of ϕ_s is as large as possible without exceeding a specified value.

Next it determines in accordance with its instructions the E, ψ, r, r', for each ion in the bunch. And finally it integrates this bunch through each cell.

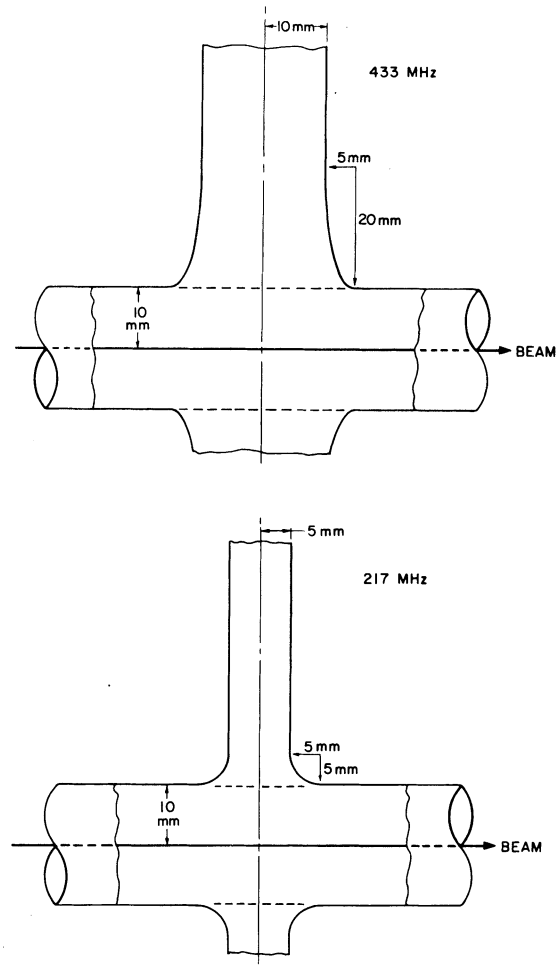

FIGURE 5 Cell structure near axis.

In the process of determining the parameters for maximum acceptance the ions are placed at random uniformly in an ellipse in $\psi - E$ space and independently at random with density proportional to r in an ellipse in $r - r'$ space, intentionally giving greater weight to the extreme excursions. After determining the optimum parameters a bunch is used in which the ions are placed uniformly at random in the five dimensional ellipse in $E - \psi - x - y - r'$ space. With x and y combined to yield r the distribution is again proportional to r.

$$P(E, \psi, r, r') = \frac{15r}{4\pi}. \tag{40}$$

Integrating out the other variables, the distribution in r is

$$Q(r) = 5r(1 - r^2)^{3/2} \tag{41}$$

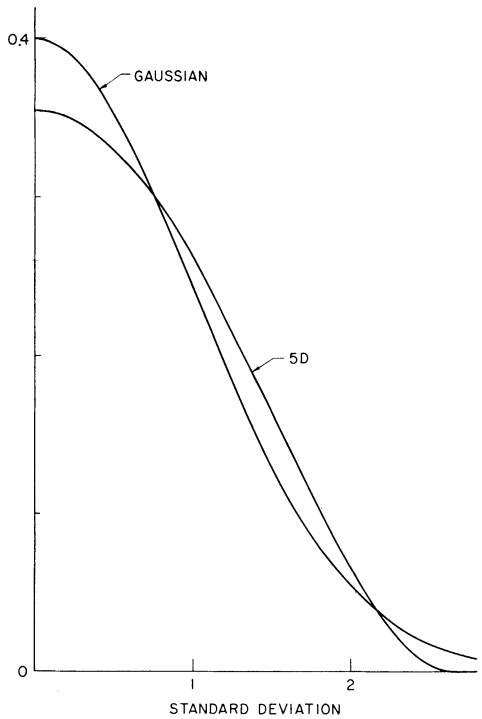

FIGURE 6 Ion distribution used, and Gaussian.

while the distribution in any one of the other three variables is

$$S(\psi) = \tfrac{15}{16}(1 - \psi^2)^2, \tag{42}$$

where ψ may be replaced by ΔE or r'. The standard deviation for this latter distribution is $\psi_{\text{rms}} = \psi_{\max} \times 7^{-1/2}$. It is compared with the Gaussian in Figure 6.

Since particles off axis generally gain more energy than those on, we find the synchronous particle being left behind. This is corrected for by adding a little energy to the synchronous particle and moving it ahead slightly in z. Typically the energy correction is 0.3% of energy gained, and the phase is 0.3 degrees per cell. At the forming of the bunch there is calculated an axis shift in ψ so that a specific ratio $R_\psi = \psi_+/\psi_-$ will obtain. This shift in degrees is maintained throughout the accelerator.

4 PARAMETRIC REPRESENTATION OF THE BEAM

For the time being we assume that erect ellipses are the input to the accelerator except for an axis shift to allow for $R_\psi \neq 1$. There are four beam parameters besides R_ψ. In their place we define four others F_z, F_r, R_z, and R_r. The change to these variables is done to facilitate the search for the best input parameters, and comparison with the theory the final results will be given in terms of both these new and conventional parameters.

$$\psi_{\max} = \psi_0 \frac{F_z}{R_z} \tag{43}$$

$$\psi'_{\max} = \frac{\psi_0}{B_z} F_z R_z \tag{44}$$

$$r_{\max} = \frac{r_0}{Q} \frac{F_r}{R_r} \tag{45}$$

$$r'_{\max} = \frac{r_0 Q}{B_r} F_r R_r. \tag{46}$$

These definitions are a consequence of Eqs. (34) and (35) and the remark closing Section 2, making the F's and R's both dimensionless and of the order of 1. Deviations from 1 reflect either the particle distribution in the beam or deviation from the theory of Section 2.

F_z^2 measures the relative z emittance and R_z^2 the relative value of the ratio $\psi'_{\max}/\psi_{\max}$. For the purpose of optimization it is useful to replace the F's and define α and ρ:

$$F_z = \alpha \cdot \rho \tag{47}$$

$$F_r = \left(\frac{\alpha}{\rho}\right)^{1/2}. \tag{48}$$

Now the total emittance is proportional to

$$A = \psi_{\max} \psi'_{\max} (r_{\max} r'_{\max})^2 = \frac{\psi_0^2 r_0^4}{B_z B_r^2} \alpha^4 \tag{49}$$

and is independent of ρ which can shift beam emittance between ψ and r. This particular definition of α was made with the intention that when α is increased as many ions would be lost due to increasing r as would be lost due to increasing ψ.

Now the beam emittance is defined by Eqs. (31) and (32) using the initial value of ϕ_s; R_ψ which shifts the $\psi = 0$ axis; R_z and R_r which change the ratios $\psi'_{\max}/\psi_{\max}$ and $r'_{\max}/r_{\max}$, respectively, without changing the magnitude of either the ψ or r emittances; ρ which shifts emittance between ψ and r without changing total; and α which multiplies everything. In hunting for the right beam to put into the accelerator, α is not an important consideration, and further, it is a fact that the $r - r'$ correlation (C_r) and the $\psi - \psi'$ correlation

(C_z) were found not very important and so were assumed zero for most of the hunt. The cross correlations such as $\psi - r$ were not considered.

In accordance with the above the beam is characterized by four important optimizable parameters, ρ, R_z, R_r, and R_ψ, and the not important but possibly nonzero correlations C_z and C_r.

5 ACCELERATOR PARAMETERS

The focusing strength, discussed in Section 2, is characterized by the value of $(n\theta_z)^2$. The length of a cell, L, is not optimizable; the shorter, the better. The magnitude of the stable phase, ϕ_s, is not optimizable without some cost input; the larger is ϕ_s, the greater the acceptance but the longer the accelerator and the more it costs.

Combined with the beam, there is another parameter qW/m the ratio of the energy available per cell to the mass of an ion. Here we expect the bigger the better and will check that by varying the ion charge q after we maximize the acceptance in the five-dimensional space in $(n\theta_z)^2$, ρ, R_z, R_r, and R_ψ. During the maximization the value of α is increased now and again to bring acceptance down to around 75% of the input beam.

Two accelerators are considered, one at 217 MHz to take the ions from $\beta = 0.03$ to $\beta = 0.075$, and another at 433 MHz to take the ions from $\beta = 0.075$ to $\beta = 0.125$. In both cases the cell length is 100 mm, the maximum potential difference per gap is 200 kV, the ion is $^{35}Cl^{+8}$, and the value of ϕ_s at which to increase n is 45°. Since the value of n is not changed, nor is the accelerator terminated except at the middle of a focusing or bunching section, the value of ϕ_s may exceed the 45° in places, and the final value of β specified may also be exceeded.

6 OPTIMUM PARAMETERS

For the purpose of optimization a more than normally sensitive distribution of ions in phase space is used as described in Section 3.

The parameters of the accelerators and associated beams are given in Table I and substantiated in Figures 7 and 8. In each case the variable parameters other than the abscissa are held constant at the value marked by the arrow in Figure 7 which refers to the 217 MHz accelerator and at the

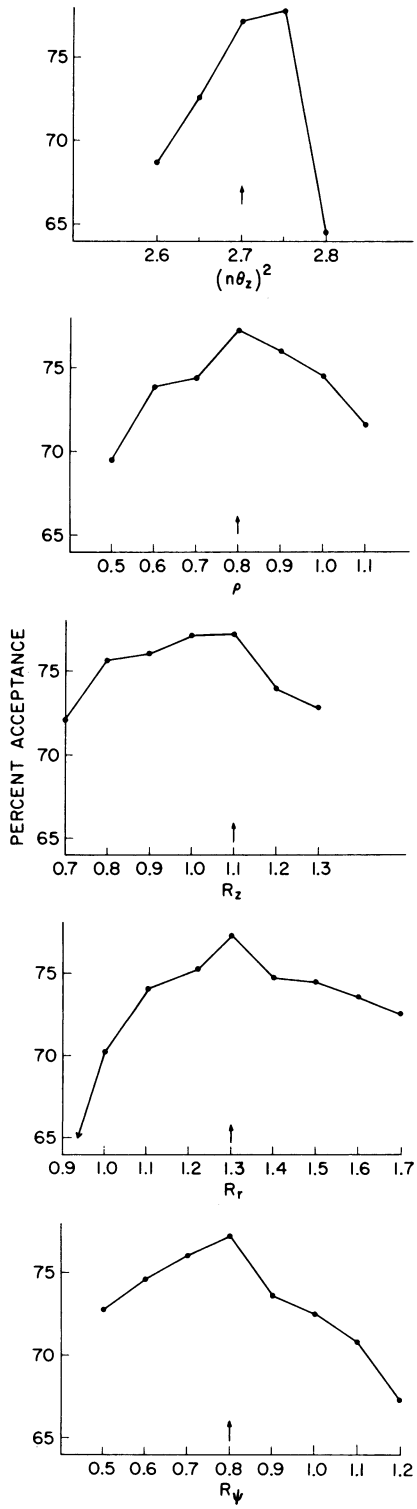

FIGURE 7 Acceptance *vs* various parameters, 217 MHz section.

TABLE I

Frequency	217	433	MHz
α	2.5	1.0	
ρ	0.8	1.3	
F_z	2.0	1.3	
F_r	1.77	0.88	
R_z	1.1	1.0	
R_r	1.3	1.3	
R_ψ	0.8	0.6	
$\Delta E/E(\psi')$	± 0.16	0.075	%
$\Delta\psi$	± 7.5	8.3	degrees
ψ axis shift	$+0.8$	$+2.1$	degrees
$\Delta\psi_+$	6.7	6.2	degrees
$\Delta\psi_-$	-8.3	-10.4	degrees
$\Delta r'$	± 3.6	1.4	mrad
r	1.5	1.4	mm
C_r	-0.3	0	
mass	35	35	amu
q	8	8	e
potential diff/gap	200	200	kV
β in	0.030	0.075	
β out	0.078	0.127	
ϕ_{max}	45	45	degrees
$(n\theta_z)^2$	2.7	2.7	
Ω_z	0.56π	0.56π	
Ω_r	0.25π	0.25π	
Q_r modulation ratio	1.43	1.43	
n initial	4	10	
ϕ_s initial	25.8	36.4	degrees
Time-of-flight factor, initial	0.50	0.44	
Number of cells	84	224	
Number of ions in the 3 bunches	2400	2400	
$\Delta E/E$ emittance	0.55	0.14	%
$\Delta\psi$ emittance	6.5	14	degrees
$\Delta r'$ emittance	1.0	1.3	mrad
r emittance	2.5	1.0	mm
Ions in emitted bunches	98.7	99.0	%

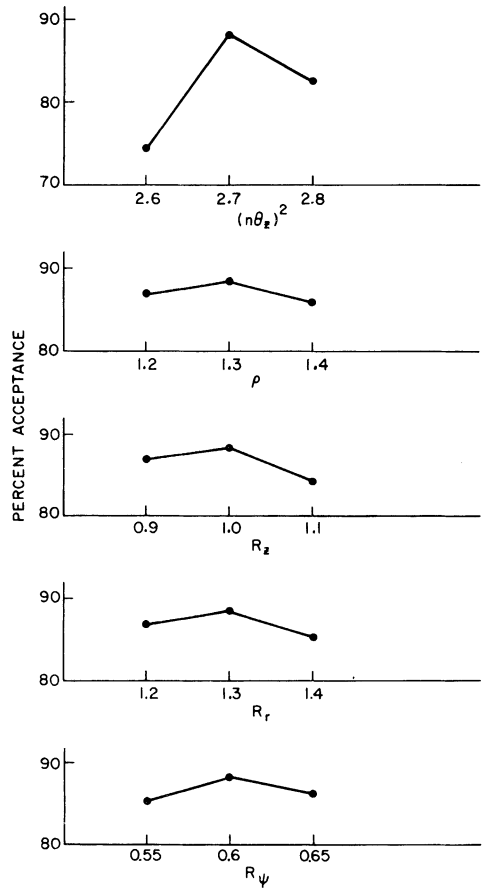

FIGURE 8 Acceptance *vs* various parameters, 433 MHz sections.

central values in Figure 8 which refers to the 433 MHz accelerator.

In Figure 7, 800 ions were used to determine each point (differences caused by using different random distributions indicate that each point should be considered to have a standard deviation of about 0.5%), the same random distribution was used for each point, the varying beam parameters merely stretching and shrinking in various directions. In Figure 7 it looks as though $(n\theta_z)^2 = 2.75$ should have been chosen, but for the small gain near the sharp drop, it appeared prudent to choose $(n\theta_z)^2 = 2.7$.

In Figure 8 only 400 ions (standard deviation $\sim 0.9\%$) determine a point. Due to the fact that this accelerator is quite long further computer time was not expended exploring for larger acceptance. Actually about 250 other points were explored, but spread in a five-dimensional space, the coverage was incomplete. Granting that there may be a better 433 MHz accelerator, there is at least one with a reasonable acceptance, and such an accelerator may be made quite long.

Table II shows how the 84 cells of the 217 MHz are arranged. The mean magnitude of ϕ_s is 34.2°.

TABLE II

Number of Cells	n	Range of ϕ_s (Degrees)
16	4	25.8 to 49.0
24	6	20.2 to 46.6
24	8	24.7 to 45.4
20	10	27.6 to 40.9
84		

As pointed out, this hunt was carried out with a type of random distribution that overestimates ion densities at large distances from the center of the multidimensional phase space. Hereafter the accelerator is tested with a uniform distribution in that multidimensional phase space.

7 VARYING OTHER PARAMETERS

We start with a beam and accelerator that are matched so that changing L, the cell length, and qW/m the energy-gain to mass ratio (by changing q only), the match is lost. The matched acceptance should be proportional to $(q/L)^{3/2}$. Figures 9 and 10

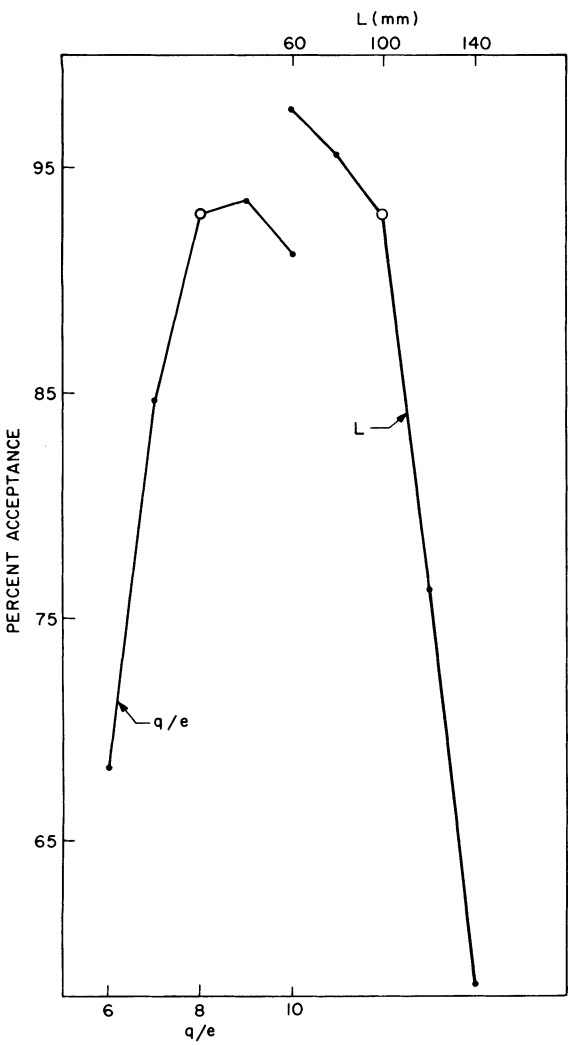

FIGURE 9 Acceptance *vs* L and q.

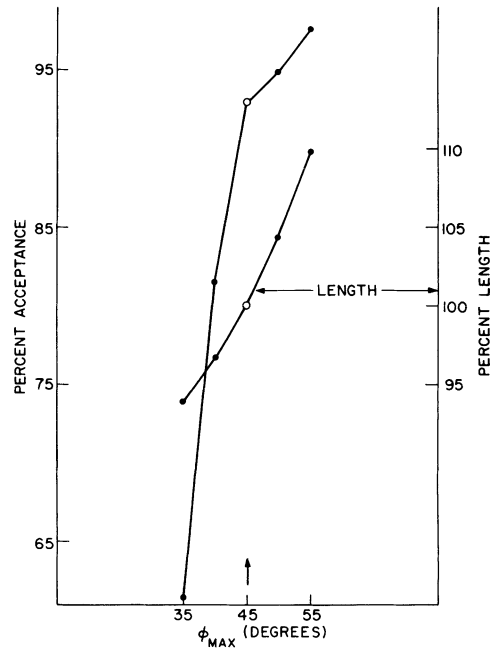

FIGURE 10 Acceptance and relative accelerator length *vs* ϕ_{max}, 217 MHz.

show the effect of changing L, q and ϕ_{max}. Besides causing mismatch, changing L merely changed the length of the accelerator but changing q caused a complete redesign of the accelerator so that Table II no longer applies. Changing ϕ_{max} did not change the front end of the accelerator, it always started with $\phi_s = 25.8°$ and $n = 4$, but the rest of the machine was redesigned causing probably a small mismatch. Figure 9 confirms that, even mismatched the shorter is L, the better. Figure 9 also shows that in order to take advantage of the expected improved acceptance for larger q, the beam and accelerator must be matched. Figure 10 shows both the increased acceptance and increased length of accelerator required due to increasing ϕ_{max}. What is plotted in these cases and those that follow is not, of course, the "acceptance of the accelerator," but a number much easier to come by, the percentage of the given beam that is accepted by the accelerator.

Correlation in the beam is generated in the computer by inserting a drift of the appropriate length and sign. Figure 11 shows that correlation in the $\psi - \psi'$ plane has little or no effect, and that a small correlation in the $r - r'$ plane of $C_r = 0.3$ is an improvement.

Recognizing that triple focusing would very likely be quite sensitive to accurate phasing, a

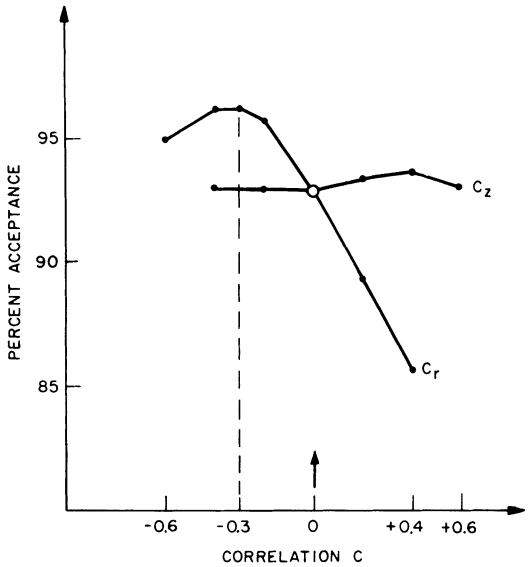

FIGURE 11 Acceptance *vs* ellipse correlations, 217 MHz.

random error in the phase setting of each cell was introduced. It appears that if this random error is such that $\Delta\phi_{\text{rms}} < 1^\circ$ the loss is insignificant as shown in Figure 12. Also considered was a constant bias. The curve's being off center is caused by the choice of value of ρ for it suggests that a little more focusing at the expense of some bunching would be in order. The width of the curve suggests

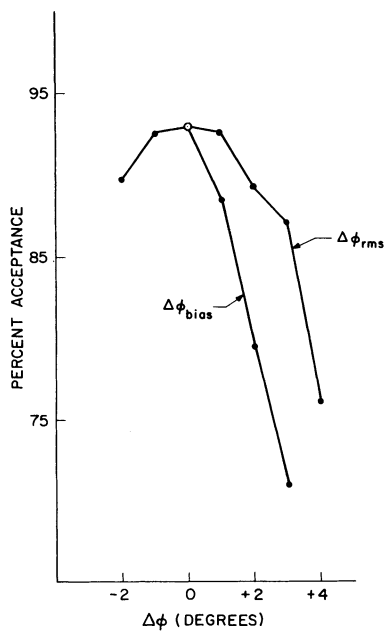

FIGURE 12 Acceptance *vs* $\Delta\phi_{\text{rms}}$ and $\Delta\phi_{\text{bias}}$, 217 MHz.

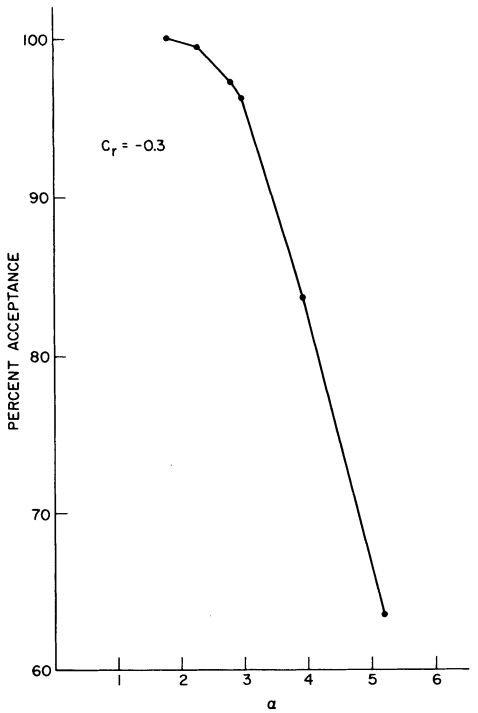

FIGURE 13 Acceptance *vs* α, 217 MHz.

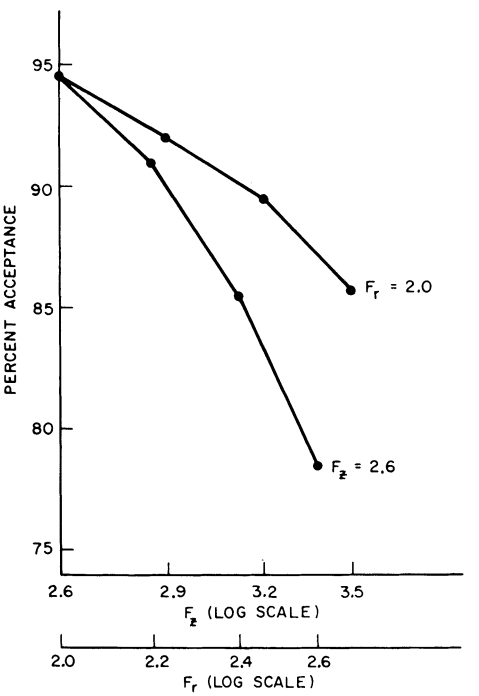

FIGURE 14 Acceptance *vs* log F_z and log F_r, 217 MHz.

that a constant bias of $|\Delta\phi| < 1^\circ$ will cause little loss.

Now adopting $C_r = -0.3$, the effect of increasing α is shown in Figure 13. And separating the effects of increasing $\psi - \psi'$ space and increasing $r - r'$ space, Figure 14 shows increasing F_z while holding F_r constant and *vice versa.*

8 FINAL RESULTS

Table I gives the parameters of the acceptance of the accelerators, the parameters of accelerators, and their emittances. The stated acceptance of, say, $\Delta\psi = \pm 7.5^\circ$ is the maximum possible under the given circumstances. With the distribution actually used the nms value is the stated maximum value divided by $(7)^{1/2}$. In the case of r which stands for two variables the rms value is the stated maximum divided by $(7/2)^{1/2}$. The results for each accelerator were based on three bunches, each with 800 ions, but based on a different set of random numbers. The quoted emittances were arrived at subjectively by drawing lines on plots, such as Figures 15 and 16, that include "almost all" of the ions. In each of these figures there are 791 O's each representing an ion's coordinates on leaving the accelerator. Unfortunately when the computer puts five or ten 0's in the same space it does not look five or ten times as dark. For instance, in Figure 15 there are 439 spaces with 0's, hence 352 multiples. Apparently the ions are quite densely grouped, but notice that there are holes in the middles of the distributions. In the other bunches at both frequencies the holes were always present although the hole in $\psi - \psi'$ space was not so apparent and in one bunch at 433 MHz could have gone unnoticed.

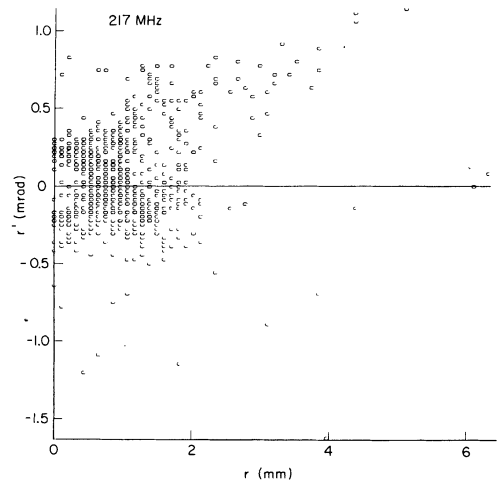

FIGURE 16 Emittance $r - r'$, 217 MHz.

Figure 17 shows where the ions are lost in the accelerators. The taller bars in the 217 MHz graph are for the loss of 23%, by an increase in α, and the shorter ones for the case reported in Table I were only 1.3% = 32 ions were lost. For the 433 MHz case, same as in Table I, 1.0% = 25 ions were lost. In the case of small losses it appears that they are more or less uniform over the last 60% to 70% of the accelerator.

To the extent that the theory[5] was intended to be believed, it is within reason. If one assumes the theory were predicting rms values, F_z, for the

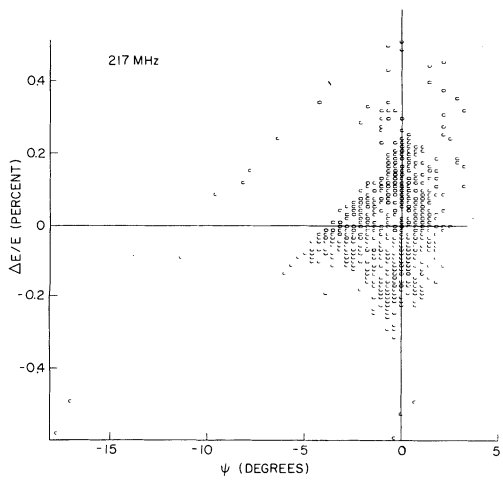

FIGURE 15 Emittance $\psi - \Delta E$, 217 MHz.

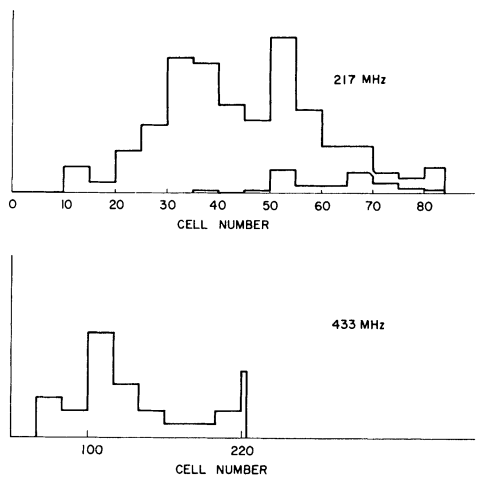

FIGURE 17 Ion loss along accelerators.

distribution explained in Section 3, should be compared with $2.6(=7^{1/2})$, R_z with 1, F_r with 2.2, R_r with 1.2, and, as stated before, R_ψ with 0.66.

The accelerators here defined may be somewhat more difficult to design than define.

REFERENCES

1. M. L. Good, *Bull. Am. Phys. Soc.* **27**, 16 (1952) and *Phys. Rev.* **92**, 538 (A) [1953].
2. L. B. Mullett, "Linear Accelerator Focussing by Periodic Changing of the Synchronous Phase Position", Harwell Report AERE GP/M, 147 (1953).
3. Ia. B. Fainberg, *Proc. CERN Symposium on High Energy Accelerators and Pion Physics*, (CERN, Geneva, 1956) p. 91.
4. A. D. Vlasov, *Theory of Linear Accelerators*, Moscow, (1965) and (English Translation) Jerusalem (1968).
5. E. E. Chambers, High Energy Physics Laboratory Report No. 653 Stanford University, Stanford, Calif. (1971).
6. I. Ben-Zvi, P. H. Ceperley and H. A. Schwettman, High Energy Physics Laboratory Report No. 731 (1974). To be published in *Particle Accelerators*.
7. H. C. Hoyt, D. D. Simmonds, W. F. Rich, *Rev. Sci. Instrum.* **37**, 755 (1966).